Nonlinear Analysis of Power System Oscillations Using Models and Measurements

Final Project Report

S-89G

Power Systems Engineering Research Center
Empowering Minds to Engineer
the Future Electric Energy System

Nonlinear Analysis of Power System Oscillations Using Models and Measurements

Final Project Report

Project Team
Vaithianathan "Mani" Venkatasubramanian, Project Leader
Washington State University

Graduate Students
Saugat Ghimire
Mohammadreza Maddipour Farrokhifard
Chad Thomas
Yuan Zhi
Washington State University

PSERC Publication 21-10

September 2021

For information about this project, contact:

Vaithianathan “Mani” Venkatasubramanian
Professor, School of Electrical Engineering and Computer Science
Washington State University
Email: mani@wsu.edu

Power Systems Engineering Research Center

The Power Systems Engineering Research Center (PSERC) is a multi-university Center conducting research on challenges facing the electric power industry and educating the next generation of power engineers. More information about PSERC can be found at the Center’s website: http://www.pserc.org.

For additional information, contact:

Power Systems Engineering Research Center
Arizona State University
527 Engineering Research Center
Tempe, Arizona 85287-5706
Phone: 480-965-1643
Fax: 480-727-2052

Notice Concerning Copyright Material

Acknowledgements

We wish to thank the industry advisors for the project, Dr. Patrick Panciatici, Dr. Florent Xavier, and Gilles Torresan from RTE for their advice and support throughout the project. Our sincere thanks are also extended to the RTE engineers, Stephane Hivart, Paul Chabas, and Charles Faure-Llorens for their constant support of the implementation and testing of the oscillation monitoring features at RTE.

Executive Summary

Hopf bifurcations can occur in power systems when a system mode experiences low damping because of changes in system operating conditions and they can lead to emergence of limit cycles and oscillations. There are two types of Hopf bifurcations, namely, supercritical and subcritical, and they are determined by the sign of a cubic normal form coefficient. This report discusses the two types of Hopf phenomena in test power system models where both types could be seen under changes in system and control parameters. The report proposes an efficient computational method for carrying out higher order center manifold and normal form calculations for a general power system model and discusses the implications of the normal form coefficients for power system dynamics. Distinguishing between subcritical versus supercritical is important since they lead to very different type of oscillatory phenomena related to unstable versus stable limit cycles respectively.

Project Publications:

[1] Y. Zhi and V. Venkatasubramanian, "Interaction of Forced Oscillation With Multiple System Modes," in *IEEE Transactions on Power Systems*, vol. 36, no. 1, pp. 518-520, Jan. 2021, doi: 10.1109/TPWRS.2020.3024407.

[2] Y. Zhi and V. Venkatasubramanian, "Analysis of Energy Flow Method for Oscillation Source Location," in *IEEE Transactions on Power Systems*, vol. 36, no. 2, pp. 1338-1349, March 2021, doi: 10.1109/TPWRS.2020.3024866.

Table of Contents

List of Figures

List of Tables

1. Introduction

1.1 Background

Oscillatory stability of a nonlinear system such as a power system is usually studied by linearizing the system dynamic model around an equilibrium point and by studying the eigenvalues of the linearized system Jacobian matrix[1]. The system is considered small-signal stable at an equilibrium if all the eigenvalues of the system matrix (usually denoted modes) evaluated at the equilibrium point have negative real parts. However, in a power system, changes in operating conditions such as from generator output variations or load changes can make one of the system modes poorly damped or even negatively damped, such as by crossing the imaginary axis into the open right half complex plane.

If a pair of complex conjugate eigenvalues transverses across the imaginary axis, this phenomenon is called a Hopf bifurcation [2],[3]. Hopf bifurcation is usually associated with nonlinear oscillatory system trajectories. In this situation, the nonlinear part of the system must be taken into consideration for further analysis of the system responses when the eigenvalues are close to the imaginary axis. Center manifold and normal form theories are two powerful tools for performing this nonlinear analysis. They together provide a systematic way to simplify dynamical systems near a Hopf bifurcation parameter value.

1.2 Overview of the Problem

Assuming all the other eigenvalues to have negative real parts, it can be shown that a two-dimensional center manifold captures the essential nonlinear features of the system dynamics associated with a poorly damped pair of complex conjugate eigenvalues[2],[3],[4]. At any Hopf bifurcation point, the normal form on the two-dimensional center manifold can be expressed in the polar form as $\dot{r} = \mu r + ar^3 + O(r^5)$, where μ is the real part of the eigenvalue of the equilibrium point, and a is the cubic normal form coefficient we are concerned about (supercritical when $a < 0$ and subcritical when $a > 0$). It can be shown that supercritical cases are related to stable limit cycles that are born as the equilibrium point becomes unstable ($\mu > 0$), which means the system trajectories will have sustained oscillations even as the mode becomes negatively damped. For the subcritical case, there is an unstable limit cycle surrounding the stable equilibrium point ($\mu < 0$), and the limit cycle will disappear as the equilibrium point becomes unstable and the system trajectory will diverge away potentially leading to tripping of equipment. Therefore, the subcritical type of Hopf is more problematic for system operations compared to the supercritical type of Hopf [4].

1.3 Proposed Solution

In this report, we will show how high order computations can be done systematically in general nonlinear differential algebraic models using center manifold theory and normal form theory [5],[6],[7] and discuss the operational implications of the phenomena for general detailed power system models such as for the 2-area-4-machine-11-bus Kundur test system[1].

1.4 Report Organization

In section 2, we will introduce the theoretical background for distinguishing between supercritical and subcritical Hopf bifurcations to provide an intuitive understanding. In section 3 we will illustrate the numerical computation process step by step for calculating the normal form coefficient “a”, which would tell us which type of Hopf it is. In section 4, we will illustrate the computations and analysis on the Kundur system. Conclusions are made in section 5.

2. Theoretical Background

2.1 Basic Concepts

In this report, the variables in bold and italic are vectors i.e $\boldsymbol{x}$; variables in bold and non-italic are matrices i.e. $\mathbf{A}$; variables neither in bold nor italic are scalars i.e. a.

For a physical system such as power system, the dynamics can be modeled by a dynamical system in the form:

$$\frac{d\boldsymbol{x}}{dt} \stackrel{\text{def}}{=} \dot{\boldsymbol{x}} = f(\boldsymbol{x}) \tag{1}$$

where $\boldsymbol{x} = \boldsymbol{x}(t) \in \mathbb{R}^n$ and $f: U \subseteq \mathbb{R}^n \to \mathbb{R}^n$ is smooth. Here we assume the network based differential-algebraic equations can be suitably simplified into the form (1) with suitable assumptions on solvability of network algebraic equations [8]. An equilibrium point say x_0 of (1) is a solution such that $f(\boldsymbol{x_0}) = 0$. A linearization of system (1) at the operating point x_0 is denoted as

$$\dot{\boldsymbol{x}} = \mathbf{A}\boldsymbol{x} \tag{2}$$

where matrix $\mathbf{A} = Df(\boldsymbol{x_0})$ is the Jacobian matrix of function $f(\boldsymbol{x})$ at $\boldsymbol{x_0}$.

It is required that a power system should be operating at an equilibrium point where it is stable under any small-scale disturbance, i.e. it must be small signal stable. This implies that all the eigenvalues of the linearized system matrix $\mathbf{A}$ have negative real parts, so that all the system states will converge to its stable equilibrium point after any small disturbance. An equilibrium point x_0 is called a *hyperbolic* equilibrium point of (1) if none of the eigenvalues of the matrix $\mathbf{A} = Df(x_0)$ have zero real part (or on the imaginary axis) [2],[3]. By this definition, a small signal equilibrium point is hyperbolic, since all its eigenvalues are negative (i.e. none of eigenvalue have zero real part).

The *Hartman-Grobman Theorem* [2],[3] states that if $x_0$is a hyperbolic equilibrium point of (1), then the local behavior of the nonlinear system (1) is topologically equivalent to the local behavior of the linearized system (2). In other words, the behavior of the nonlinear system in the vicinity of the equilibrium is determined by the behavior of the linearized system. Moreover, the behavior of the system in the vicinity of the equilibrium can be characterized by the Eigen space of the Jacobian matrix $\mathbf{A}$. For example, the trajectory will approach the equilibrium in the directions given by eigenvectors whose eigenvalues have negative real parts, while diverging in the directions given by eigenvectors whose eigenvalues have positive real parts. Therefore, the Hartman-Grobman Theorem completely solves the problem of determining the stability and qualitative behavior in the vicinity of a hyperbolic equilibrium point of nonlinear system, i.e. we could study the nonlinear system behavior by using its linearized system in the vicinity of a hyperbolic equilibrium point.

2.2 Center Manifold Theorem

As the system operating condition changes (for instance, from changes in generator outputs, load demands, and topology), if one or more eigenvalues of the linearized system have zero real parts (or very close to the imaginary axis), then it is no longer valid to study the system behavior via the linearized system. In this case, the Hartman-Grobman Theorem is not applicable any more. At this point, *Center Manifold Theorem* provides the methodology for analyzing the system qualitative behavior in the vicinity of an equilibrium point with zero real part eigenvalues (non-hyperbolic equilibrium point). In this case, the local dynamics near the equilibrium is determined by its behavior on an associated center manifold [2],[3]. Center manifold theory enables us to reduce the dimension of the state space onto the center manifold (which has the same dimension as the number of zero real part eigenvalues). That is, we only need to analyze a much smaller dimensional dynamical system whose behavior determines the original large system qualitatively.

Consider a dynamical system in the form of

$$\begin{cases} \dot{\boldsymbol{x}} = \mathbf{C}\boldsymbol{x} + F(\boldsymbol{x}, \boldsymbol{y}) \\ \dot{\boldsymbol{y}} = \mathbf{P}\boldsymbol{y} + G(\boldsymbol{x}, \boldsymbol{y}) \end{cases} \tag{3}$$

where $(\boldsymbol{x}, \boldsymbol{y}) \in \mathbb{R}^c \times \mathbb{R}^s$**,** and $\mathbf{C} \in \mathbb{R}^{c \times c}$ is a square matrix with all its eigenvalues having zero real parts, and $\mathbf{P} \in \mathbb{R}^{s \times s}$ is a square matrix with all its eigenvalues having negative real parts. Assuming $(\boldsymbol{x}, \boldsymbol{y}) = (\mathbf{0}, \mathbf{0})$ is an equilibrium point of the system satisfying $F(\mathbf{0}, \mathbf{0}) = G(\mathbf{0}, \mathbf{0}) = \mathbf{0}$ and $DF(\mathbf{0}, \mathbf{0}) = DG(\mathbf{0}, \mathbf{0}) = \mathbf{0}$**.** Then the center manifold is defined as:

$$W_{loc}^{c}(\mathbf{0}) = \begin{Bmatrix} (\boldsymbol{x}, \boldsymbol{y}) \in \mathbb{R}^c \times \mathbb{R}^s \mid \boldsymbol{y} = h(\boldsymbol{x}), \\ |\boldsymbol{x}| < \delta, h(\mathbf{0}) = \mathbf{0}, Dh(\mathbf{0}) = \mathbf{0} \end{Bmatrix} \tag{4}$$

And the flow on the center manifold $W_{loc}^{c}(\mathbf{0})$ is defined by the system of differential equations:

$$\dot{\boldsymbol{x}} = \mathbf{C}\boldsymbol{x} + F\big(\boldsymbol{x}, h(\boldsymbol{x})\big) \tag{5}$$

$\forall\, \boldsymbol{x} \in \mathbb{R}^{\boldsymbol{c}}$ with $|\boldsymbol{x}| < \delta$**.** Furthermore, the function $h(\boldsymbol{x})$ is obtained by solving:

$$Dh(\boldsymbol{x})\big[\mathbf{C}\boldsymbol{x} + F\big(\boldsymbol{x}, \boldsymbol{h}(\boldsymbol{x})\big)\big] - \mathbf{P}h(\boldsymbol{x}) - \boldsymbol{G}\big(\boldsymbol{x}, h(\boldsymbol{x})\big) = \mathbf{0} \tag{6}$$

Now, after we got the center manifold, we could just study the system $\dot{\boldsymbol{x}} = \mathbf{C}\boldsymbol{x} + \boldsymbol{F}\big(\boldsymbol{x}, \boldsymbol{h}(\boldsymbol{x})\big)$**,** which is a c-dimensional system of dimension much less than that of the original $c + s$. For Hopf bifurcation analysis, the center manifold is two-dimensional with $c = 2$.

2.3 Normal Form Theory

Furthermore, normal form is the tool we are applying next to further simplify nonlinear part $F(\boldsymbol{x})$ of the system on the center manifold (5). It is accomplished by a series of nonlinear transformations of coordinates in the form of

$$\boldsymbol{x} = \boldsymbol{y} + h(\boldsymbol{y}) \tag{7}$$

where $h(\boldsymbol{y}) = O(|\boldsymbol{y}|^{\mathbf{2}})$ as $|\boldsymbol{y}| \to \mathbf{0}$**.** Note here the nonlinear function $h(\boldsymbol{y})$ is different from the one in center manifold theorem (5). The transformations are used to eliminate as many higher order terms as possible so that we can analyze a "minimal" set of higher order terms which are then denoted as the *normal form* [2],[3]. After a series of such nonlinear transformations, the system on the center manifold would be ended up in the form of

$$\dot{\boldsymbol{y}} = \mathbf{C}\boldsymbol{y} + F_2^r(\boldsymbol{y}) + F_3^r(\boldsymbol{y}) + \cdots + F_{r-1}^r(\boldsymbol{y}) + \boldsymbol{O}(|\boldsymbol{y}|^r) \tag{8}$$

where terms $F_k^r(y)$ are referred to as resonance terms in monomials of y in order k. The detailed process is shown in the section below.

2.4 Hopf Bifurcations

When system parameters are varied, changes may occur in the qualitative structure of the dynamics for certain parameter values. These changes are called *bifurcations* and the parameter values are called *bifurcation points.*

Particularly, if a system has a pair of complex conjugate eigenvalues on imaginary axis, then we say the system undergoes a Hopf *bifurcation* [3],[4],[9]. Then, the third order approximation of the system near the equilibrium on its center manifold can be stated as:

$$\begin{cases}\dot{x} = \mu x - \omega y + (ax - by)(x^2 + y^2) \\ \dot{y} = \omega x + \mu y + (bx + ay)(x^2 + y^2)\end{cases} \tag{9}$$

where *x* and *y* are the local coordinates on the 2-dimensional center manifold. Furthermore, letting $x = rcos\theta$ and $y = rsin\theta$, the above equation can be written in polar coordinates which will make it easier to analyze:

$$\begin{cases}\dot{r} = \mu r + ar^3 \\ \dot{\theta} = \omega + br^2\end{cases} \tag{10}$$

Then we have four different cases: two major cases I and II, where $a > 0$ and $a < 0$. For each major case, we also need to discuss two minor cases A and B, where $\mu > 0$ and $\mu < 0$.

2.4.1 Case IA: $\boldsymbol{a > 0, \mu > 0}$

In this case the system only has an unstable equilibrium point at $r = 0$, which corresponds to the origin in the $x - y$ coordinates. Since $\dot{\theta} = \omega + br^2$, the system trajectory will spiral outwards from the origin.

2.4.2 Case IB: $\boldsymbol{a > 0, \mu < 0}$

In this case, solving equation $\mu r + ar^3 = 0$ for equilibrium point we will get 3 solutions: $r = -\sqrt{-\frac{\mu}{a}} < 0$, $r = \sqrt{-\frac{\mu}{a}} > 0$ and $r = 0$. Since in polar coordinates $r < 0$ is meaningless, so solution $r = -\sqrt{-\frac{\mu}{a}} < 0$ can be discarded. As for $r = \sqrt{-\frac{\mu}{a}}$, its eigenvalue is $-2\mu > 0$, so it is unstable. In $x - y$ coordinates, it is an unstable closed orbit or limit cycle. As for $r = 0$, its eigenvalue is $\mu < 0$, so the origin is an unstable equilibrium point where trajectory will spiral away from the origin. A special case is for $\mu = 0$. It is easily known that the system only has an unstable equilibrium point at the origin where all trajectories are spiral outwards from it.

Therefore, the above analysis for can be summarized into the bifurcation diagram shown in Figure 2.1. This type of bifurcation is called *subcritical Hopf bifurcation*, whose signature is the birth (or annihilation) of unstable limit cycles.

2.4.3 Case IIA: $a < 0, \mu > 0$

This case is similar to Case IB. We would have 2 meaningful equilibrium point by solving equation $\mu r + ar^3 = 0$: $r = \sqrt{-\frac{\mu}{a}} > 0$ and $r = 0$. As for $r = \sqrt{-\frac{\mu}{a}} > 0$, its eigenvalue is $-2\mu < 0$, so it is a stable limit cycle in $x - y$ coordinates. As for $r = 0$, its eigenvalue is $\mu > 0$, so the origin is a stable equilibrium point so that the trajectories will spiral toward the origin as dictated by the nonlinear dynamics.

2.4.4 Case IIB: $a < 0, \mu < 0$

This case is similar to Case IA. The system only has a stable equilibrium point at origin $r = 0$, where the system trajectory will spiral inward to the origin. For $\mu = 0$. It is easily known that the system only has a stable equilibrium point at the origin where all trajectories are spiral inwards to it.

The bifurcation plot is summarized as shown in Figure 2.2. This kind of bifurcation is called *supercritical Hopf bifurcation*, which is signified by the birth (or annihilation) of stable limit cycles.

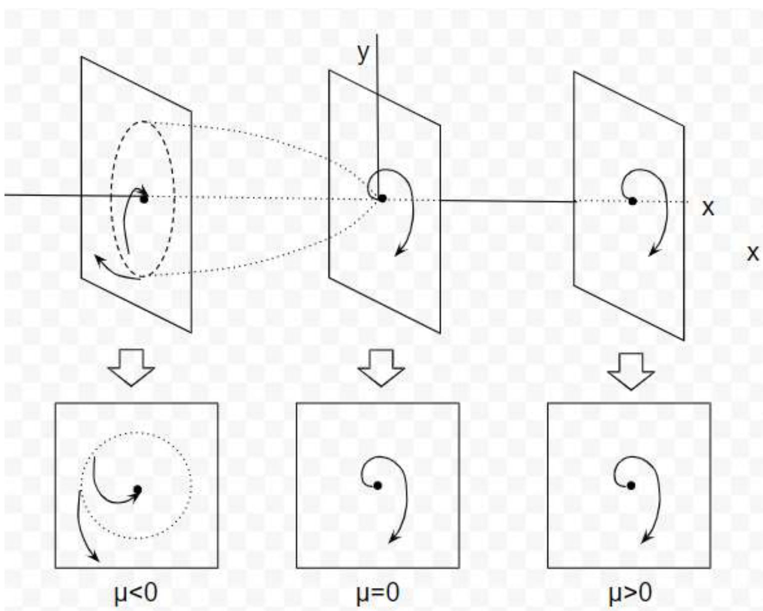

Figure 2.1 Bifurcation diagram for subcritical Hopf bifurcation ($a > 0$)

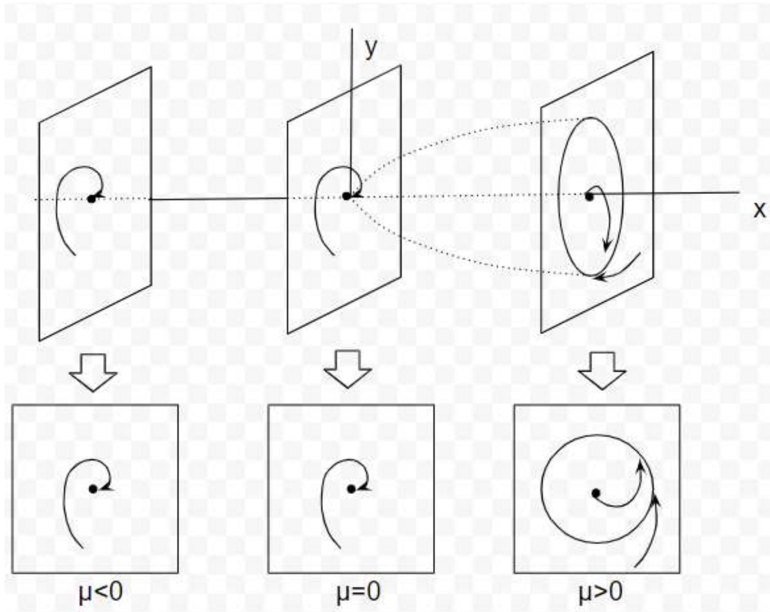

Figure 2.2 Bifurcation diagram for supercritical Hopf bifurcation ($a < 0$)

From the above analysis, we can see that the sign of parameter a in the system plays a crucial rule in distinguishing between subcritical ($a > 0$) and supercricial ($a < 0$) cases. If a system has already been reduced onto its center manifold, i.e. in a two dimensional system of the form:

$$\begin{pmatrix} \dot{x} \\ \dot{y} \end{pmatrix} = \begin{pmatrix} 0 & -\omega \\ \omega & 0 \end{pmatrix} \begin{pmatrix} x \\ y \end{pmatrix} + \begin{pmatrix} f(x,y) \\ g(x,y) \end{pmatrix} \tag{11}$$

with $f(0,0) = g(0,0) = 0$ and $Df(0,0) = Dg(0,0) = 0$, the value of a could be calculated by[2]:

$$a = \frac{1}{16}\left[f_{xxx} + f_{xyy} + g_{xxy} + g_{yyy}\right] + \frac{1}{16\omega}\begin{bmatrix} f_{xy}\left(f_{xx} + f_{yy}\right) - g_{xy}\left(g_{xx} + g_{yy}\right) \\ -f_{xx}g_{xx} + f_{yy}g_{yy} \end{bmatrix} \tag{12}$$

3. Numerical Computation of Hopf Bifurcation Third Order Normal Form Coefficient

In this section, we will show an efficient computational procedure for calculating the third order normal form coefficient a for the Hopf bifurcation. We are assuming that the system we are analyzing has a pair of complex conjugate eigenvalues on the imaginary axis, e.g. $\pm j\omega$ at some parameter value $\mu = \mu_0$.

We start from the whole system equation denoted as:

$$\dot{\boldsymbol{z}} = f(\boldsymbol{z}), \quad f(\boldsymbol{z_0}) = 0, \quad \boldsymbol{z} \in \mathbb{R}^n \tag{13}$$

where $\boldsymbol{z_0}$ is an equilibrium point of the system. Let $\Delta\boldsymbol{z} = \boldsymbol{z} - \boldsymbol{z_0}$ then the linearized system in the vicinity of $\boldsymbol{z_0}$ can be express in Taylor series as:

$$\dot{\Delta\boldsymbol{z}} = \mathbf{J}\Delta\boldsymbol{z} + \mathbf{Z_2}\boldsymbol{B}_z^2 + \mathbf{Z_3}\boldsymbol{B}_z^3 + \cdots \tag{14}$$

$$\boldsymbol{B}_z^2 = \Delta\boldsymbol{z} \otimes \Delta\boldsymbol{z} \tag{15}$$

$$\boldsymbol{B}_z^3 = \Delta\boldsymbol{z} \otimes \Delta\boldsymbol{z} \otimes \Delta\boldsymbol{z} \tag{16}$$

where matrix $\mathbf{J}$ is the Jacobian matrix and matrix $\mathbf{Z_2}$ and $\mathbf{Z_3}$ are 2nd and 3rd order derivatives of function f with respect to $\Delta\boldsymbol{z}$ at $\boldsymbol{z_0}$. $\otimes$ stands for the Kronecker product.

Now we could apply a coordinate transformation matrix $\mathbf{Q}$ to change $\mathbf{J}$ into Jordon canonical form, let

$$\boldsymbol{w} = \mathbf{Q}\Delta\boldsymbol{z} \tag{17}$$

we could get:

$$\dot{\boldsymbol{w}} = \mathbf{QJQ^{-1}}\boldsymbol{w} + \mathbf{W_2}\boldsymbol{B}_w^2 + \mathbf{W_3}\boldsymbol{B}_w^3 \tag{18}$$

Here

$$\mathbf{QJQ^{-1}} = \begin{bmatrix} \boldsymbol{\Lambda}_c & \mathbf{0} \\ \mathbf{0} & \boldsymbol{\Lambda}_s \end{bmatrix} \tag{19}$$

$$\boldsymbol{B}_w^2 = \boldsymbol{w} \otimes \boldsymbol{w} = (\mathbf{Q} \otimes \mathbf{Q})(\boldsymbol{\Delta z} \otimes \boldsymbol{\Delta z}) = (\boldsymbol{Q} \otimes \boldsymbol{Q})\boldsymbol{B}_z^2 \tag{20}$$

$$\begin{aligned} \boldsymbol{B}_w^3 = \boldsymbol{w} \otimes \boldsymbol{w} \otimes \boldsymbol{w} &= (\mathbf{Q} \otimes \mathbf{Q} \otimes \mathbf{Q})(\boldsymbol{\Delta z} \otimes \boldsymbol{\Delta z} \otimes \boldsymbol{\Delta z}) \\ &= (\mathbf{Q} \otimes \mathbf{Q} \otimes \mathbf{Q})\boldsymbol{B}_z^3 \end{aligned} \tag{21}$$

where matrix $\boldsymbol{\Lambda_s}$ is a diagonal matrix has all its eigenvalues with negative real parts; matrix $\boldsymbol{\Lambda_c}$ is a diagonal matrix has all its eigenvalues with zero real parts, i.e. on the imaginary axis.

If we denote $\boldsymbol{w} = \begin{bmatrix} \boldsymbol{u} \\ \boldsymbol{v} \end{bmatrix}$, then the system can be expresses as

$$\begin{cases} \dot{\boldsymbol{u}} = \boldsymbol{\Lambda_c}\boldsymbol{u} + f_2(\boldsymbol{u},\boldsymbol{v}) + f_3(\boldsymbol{u},\boldsymbol{v}) + \cdots \\ \dot{\boldsymbol{v}} = \boldsymbol{\Lambda_s}\boldsymbol{v} + g_2(\boldsymbol{u},\boldsymbol{v}) + g_3(\boldsymbol{u},\boldsymbol{v}) + \cdots \end{cases} \tag{22}$$

where $\boldsymbol{u} \in \mathbb{R}^c$ and $\boldsymbol{v} \in \mathbb{R}^s$, $c + s = n$.

Functions $f_i(\boldsymbol{u},\boldsymbol{v})$ and $g_i(\boldsymbol{u},\boldsymbol{v})$ are consist of i^{th} order polynomial terms of $\boldsymbol{u},\boldsymbol{v}$. For example,

$$\begin{aligned} f_2(\boldsymbol{u},\boldsymbol{v}) &= \mathbf{F}_2^{\mathbf{uu}}(\boldsymbol{u} \otimes \boldsymbol{u}) + \mathbf{F}_2^{\mathbf{uv}}(\boldsymbol{u} \otimes \boldsymbol{v}) + \mathbf{F}_2^{\mathbf{vv}}(\boldsymbol{v} \otimes \boldsymbol{v}) \\ &= \mathbf{F}_2^{\mathbf{uu}}\boldsymbol{B}_u^2 + \mathbf{F}_2^{\mathbf{uv}}\boldsymbol{B}_{uv} + \mathbf{F}_2^{\mathbf{vv}}\boldsymbol{B}_v^2 \end{aligned} \tag{23}$$

$$\begin{aligned} g_2(\boldsymbol{u},\boldsymbol{v}) &= \mathbf{G}_2^{\mathbf{uu}}(\boldsymbol{u} \otimes \boldsymbol{u}) + \mathbf{G}_2^{\mathbf{uv}}(\boldsymbol{u} \otimes \boldsymbol{v}) + \mathbf{G}_2^{\mathbf{vv}}(\boldsymbol{v} \otimes \boldsymbol{v}) \\ &= \mathbf{G}_2^{\mathbf{uu}}\boldsymbol{B}_u^2 + \mathbf{G}_2^{\mathbf{uv}}\boldsymbol{B}_{uv} + \mathbf{G}_2^{\mathbf{vv}}\boldsymbol{B}_v^2 \end{aligned} \tag{24}$$

In a similar manner:

$$f_3(\boldsymbol{u},\boldsymbol{v}) = \mathbf{F}_3^{\mathbf{uuu}}\boldsymbol{B}_{\boldsymbol{u}}^{\mathbf{3}} + \mathbf{F}_3^{\mathbf{uuv}}\boldsymbol{B}_{\boldsymbol{uuv}} + \mathbf{F}_3^{\mathbf{uvv}}\boldsymbol{B}_{\boldsymbol{uvv}} + \mathbf{F}_3^{\mathbf{vvv}}\boldsymbol{B}_{\boldsymbol{v}}^{\mathbf{3}} \tag{25}$$

$$g_3(\boldsymbol{u},\boldsymbol{v}) = \mathbf{G}_3^{\mathbf{uuu}}\boldsymbol{B}_{\boldsymbol{u}}^{\mathbf{3}} + \mathbf{G}_3^{\mathbf{uuv}}\boldsymbol{B}_{\boldsymbol{uuv}} + \mathbf{G}_3^{\mathbf{uvv}}\boldsymbol{B}_{\boldsymbol{uvv}} + \mathbf{G}_3^{\mathbf{vvv}}\boldsymbol{B}_{\boldsymbol{v}}^{\mathbf{3}} \tag{26}$$

Now our objective is:

1. Calculate center manifold of the equilibrium point, to simply the system onto its center manifold.
2. Calculate the normal form of the system up to its 3rd order (cubic) terms to get the a coefficient in the Hopf bifurcation normal form.
3. Analyze bifurcation based on the normal form.

3.1 Center manifold calculations

Since we only need the system normal form up to its 3rd order terms, so a center manifolds up to quadratic terms will be enough. We could express the center manifold as:

$$\boldsymbol{v} = \mathbf{H}_{\mathbf{c2}}(\boldsymbol{u} \otimes \boldsymbol{u}) = \mathbf{H}_{\mathbf{c2}}\boldsymbol{B}_{\boldsymbol{u}}^{\mathbf{2}} \tag{27}$$

then we will get

$$\dot{\boldsymbol{v}} = \mathbf{H}_{\mathbf{c2}}D\boldsymbol{B}_{\boldsymbol{u}}^{\mathbf{2}} \cdot \dot{\boldsymbol{u}} \tag{28}$$

Then substitute this equation into the equation of $\dot{\boldsymbol{u}}$, and equate the terms of $\boldsymbol{B}_{\boldsymbol{u}}^{\mathbf{2}}$ on both sides, we will get:

$$\boldsymbol{\Lambda}_s\mathbf{H}_{\mathbf{c2}}\boldsymbol{B}_{\boldsymbol{u}}^{\mathbf{2}} - \mathbf{H}_{\mathbf{c2}}D\boldsymbol{B}_{\boldsymbol{u}}^{\mathbf{2}} \cdot \boldsymbol{\Lambda}_{\mathbf{c}}\boldsymbol{u} = -\mathbf{G}_2^{\mathbf{uu}}\boldsymbol{B}_{\boldsymbol{u}}^{\mathbf{2}} \tag{29}$$

Here $D\boldsymbol{B}_{\boldsymbol{u}}^{\mathbf{2}} = D(\boldsymbol{u} \otimes \boldsymbol{u}) = \boldsymbol{u} \otimes \mathbf{I} + \mathbf{I} \otimes \boldsymbol{u}$, thus

$$D\boldsymbol{B}_{\boldsymbol{u}}^{\mathbf{2}} \cdot \boldsymbol{\Lambda}_{\mathbf{c}}\boldsymbol{u} = \left((\mathbf{I} \otimes \boldsymbol{\Lambda}_{\mathbf{c}}) + \begin{bmatrix} \mathbf{I} \otimes \boldsymbol{\Lambda}_{c1} \\ \vdots \\ \mathbf{I} \otimes \boldsymbol{\Lambda}_{cn} \end{bmatrix} \right) \boldsymbol{B}_{\boldsymbol{u}}^{\mathbf{2}} \stackrel{\text{def}}{=} \mathbf{C}_2\boldsymbol{B}_{\boldsymbol{u}}^{\mathbf{2}} \tag{30}$$

where $\boldsymbol{\Lambda}_{c1}, \dots, \boldsymbol{\Lambda}_{cn}$ are rows of matrix $\boldsymbol{\Lambda}_{\mathbf{c}}$

Then we could get $\mathbf{H}_{\mathbf{C2}}$ by solving the matrix equation

$$\boldsymbol{\Lambda}_{\mathbf{s}}\mathbf{H}_{\mathbf{c2}} - \mathbf{H}_{\mathbf{c2}}\mathbf{C}_2 = -\mathbf{G}_2^{\mathbf{uu}} \tag{31}$$

Once we got the quadratic center manifold $\boldsymbol{v} = \mathbf{H}_{\mathbf{c2}}\boldsymbol{B}_{\boldsymbol{u}}^{\mathbf{2}}$, we need to substitute it into the system to get the approximation of the flow on the center manifold, we will have:

$$\dot{\boldsymbol{u}} = \boldsymbol{\Lambda}_{\mathbf{c}}\boldsymbol{u} + f_2(\boldsymbol{u}, \mathbf{H}_{\mathbf{c2}}\boldsymbol{B}_{\boldsymbol{u}}^{\mathbf{2}}) + f_3(\boldsymbol{u}, \mathbf{H}_{\mathbf{c2}}\boldsymbol{B}_{\boldsymbol{u}}^{\mathbf{2}}) + \cdots \tag{32}$$

Now we can plug $\boldsymbol{v} = \mathbf{H}_{\mathbf{c2}}\boldsymbol{B}_{\boldsymbol{u}}^{\mathbf{2}}$ into the equation of $f_2(\boldsymbol{u},\boldsymbol{v})$ to update the 2nd and higher order terms on the right hand side.

$$\begin{aligned} f_2(\boldsymbol{u}, \mathbf{H}_{\mathbf{c2}}\boldsymbol{B}_{\boldsymbol{u}}^{\mathbf{2}}) &= \mathbf{F}_2^{\mathbf{uu}}\boldsymbol{B}_{\boldsymbol{u}}^{\mathbf{2}} + \mathbf{F}_2^{\mathbf{uv}}(\boldsymbol{u} \otimes \mathbf{H}_{\mathbf{c2}}\boldsymbol{B}_{\boldsymbol{u}}^{\mathbf{2}}) + \\ &\quad \mathbf{F}_2^{\mathbf{vv}}(\mathbf{H}_{\mathbf{c2}}\boldsymbol{B}_{\boldsymbol{u}}^{\mathbf{2}} \otimes \mathbf{H}_{\mathbf{c2}}\boldsymbol{B}_{\boldsymbol{u}}^{\mathbf{2}}) \\ &= \mathbf{F}_2^{\mathbf{uu}}\boldsymbol{B}_{\boldsymbol{u}}^{\mathbf{2}} + \mathbf{F}_2^{\mathbf{uv}}(\mathbf{I} \otimes \mathbf{H}_{\mathbf{c2}})(\boldsymbol{u} \otimes \boldsymbol{B}_{\boldsymbol{u}}^{\mathbf{2}}) + \\ &\quad \mathbf{F}_2^{\mathbf{vv}}(\mathbf{H}_{\mathbf{c2}} \otimes \mathbf{H}_{\mathbf{c2}})(\boldsymbol{B}_{\boldsymbol{u}}^{\mathbf{2}} \otimes \boldsymbol{B}_{\boldsymbol{u}}^{\mathbf{2}}) \\ &= \mathbf{F}_2^{\mathbf{uu}}\boldsymbol{B}_{\boldsymbol{u}}^{\mathbf{2}} + \mathbf{F}_2^{\mathbf{uv}}(\mathbf{I} \otimes \mathbf{H}_{\mathbf{c2}})\boldsymbol{B}_{\boldsymbol{u}}^{\mathbf{3}} + O(\boldsymbol{u}^{\mathbf{4}}) \end{aligned} \tag{33}$$

In a similar manner for $f_3(u,v)$ we get:

$$f_3(\boldsymbol{u}, \mathbf{H}_{\mathbf{c2}}\boldsymbol{B}_{\boldsymbol{u}}^{\mathbf{2}}) = \mathbf{F}_{\mathbf{3}}^{\mathbf{uuu}}\boldsymbol{B}_{\boldsymbol{u}}^{\mathbf{3}} + O(\boldsymbol{u}^{\mathbf{4}}) \tag{34}$$

Combine (33) and (34) into (32), center manifold up to third order can be expressed as:

$$\dot{\boldsymbol{u}} = \boldsymbol{\Lambda}_{\mathbf{c}}\boldsymbol{u} + \mathbf{F}_{\mathbf{2}}^{\mathbf{uu}}\boldsymbol{B}_{\boldsymbol{u}}^{\mathbf{2}} + \underbrace{\begin{pmatrix} \mathbf{F}_{\mathbf{2}}^{\mathbf{uv}}(\mathbf{I} \otimes \mathbf{H}_{\mathbf{c2}}) \\ +\mathbf{F}_{\mathbf{3}}^{\mathbf{uuu}} \end{pmatrix}}_{\mathbf{F}_{\mathbf{3c}}^{\mathbf{u}}} \boldsymbol{B}_{\boldsymbol{u}}^{\mathbf{3}} + O(\boldsymbol{u}^{\mathbf{4}}) \tag{35}$$

Now we can see the original n dimensional system has been reduced into a c dimensional system. Usually c is much smaller than n, so the center manifold simplifies the system we need to analyze. Now from here we need to calculate the normal form.

3.2 Quadratic normal form calculations

From previous section we see how center manifold theory could simplify the system we need to analyze. Now the normal form is to simplify the center manifold further, which is what we are going to show in this section. Basically, it is accomplished by introducing a series of nonlinear transformations to the system on the center manifold.

This can be accomplished by the nonlinear transformation in the form:

$$\boldsymbol{u} = \boldsymbol{y} + \mathbf{H}_{\mathbf{2n}}\boldsymbol{B}_{\boldsymbol{y}}^{\mathbf{2}} \tag{36}$$

Then by plugging it into the center manifold equation (35), we will get:

$$\begin{aligned} \dot{\boldsymbol{y}} &= \left(\mathbf{I} + \mathbf{H}_{\mathbf{2n}}D\boldsymbol{B}_{\boldsymbol{y}}^{\mathbf{2}}\right)^{-1} \begin{bmatrix} \boldsymbol{\Lambda}_{\mathbf{c}}\boldsymbol{y} + \boldsymbol{\Lambda}_{\mathbf{c}}\mathbf{H}_{\mathbf{2n}}\boldsymbol{B}_{\boldsymbol{y}}^{\mathbf{2}} + \\ \mathbf{F}_{\mathbf{2}}^{\mathbf{uu}}\boldsymbol{B}_{\boldsymbol{y}}^{\mathbf{2}} + O(\boldsymbol{y}^3) \end{bmatrix} \\ &= \boldsymbol{\Lambda}_{\mathbf{c}}\boldsymbol{y} + \begin{pmatrix} \boldsymbol{\Lambda}_{\mathbf{c}}\mathbf{H}_{\mathbf{2n}}\boldsymbol{B}_{\boldsymbol{y}}^{\mathbf{2}} + \mathbf{F}_{\mathbf{2}}^{\mathbf{uu}}\boldsymbol{B}_{\boldsymbol{y}}^{\mathbf{2}} \\ -\mathbf{H}_{\mathbf{2n}}D\boldsymbol{B}_{\boldsymbol{y}}^{\mathbf{2}} \cdot \boldsymbol{\Lambda}_{\mathbf{c}}\boldsymbol{y} \end{pmatrix} + O(\boldsymbol{y}^3) \end{aligned} \tag{37}$$

Here we approximated $\left(\mathbf{I} + \mathbf{H}_{\mathbf{2n}}D\boldsymbol{B}_{\boldsymbol{y}}^{\mathbf{2}}\right)^{-1} \approx \mathbf{I} - \mathbf{H}_{\mathbf{2n}}D\boldsymbol{B}_{\boldsymbol{y}}^{\mathbf{2}} + O(\boldsymbol{y}^{\mathbf{2}})$**.** Now the 2nd order terms are given by $\boldsymbol{\Lambda}_{\mathbf{c}}\mathbf{H}_{\mathbf{2n}}\boldsymbol{B}_{\boldsymbol{y}}^{\mathbf{2}} + \mathbf{F}_{\mathbf{2}}^{\mathbf{uu}}\boldsymbol{B}_{\boldsymbol{y}}^{\mathbf{2}} - \mathbf{H}_{\mathbf{2n}}D\boldsymbol{B}_{\boldsymbol{y}}^{\mathbf{2}} \cdot \boldsymbol{\Lambda}_{\mathbf{c}}\boldsymbol{y}$**,** which is what we want to simply as much as possible. This is accomplished by solving for an appropriate matrix $\mathbf{H}_{\mathbf{2n}}$**.** We notice that $D\boldsymbol{B}_{\boldsymbol{y}}^{\mathbf{2}} \cdot \boldsymbol{\Lambda}_{\mathbf{c}}\boldsymbol{y} = \mathbf{C}_{\mathbf{2}}\boldsymbol{B}_{\boldsymbol{y}}^{\mathbf{2}}$ as in (30), so we could get:

$$\begin{aligned} &\boldsymbol{\Lambda}_{\mathbf{c}}\mathbf{H}_{\mathbf{2n}}\boldsymbol{B}_{\boldsymbol{y}}^{\mathbf{2}} + \mathbf{F}_{\mathbf{2}}^{\mathbf{uu}}\boldsymbol{B}_{\boldsymbol{y}}^{\mathbf{2}} - \mathbf{H}_{\mathbf{2n}}D\boldsymbol{B}_{\boldsymbol{y}}^{\mathbf{2}} \cdot \boldsymbol{\Lambda}_{\mathbf{c}}\boldsymbol{y} \\ &= (\boldsymbol{\Lambda}_{\mathbf{c}}\mathbf{H}_{\mathbf{2n}} - \mathbf{H}_{\mathbf{2n}}\mathbf{C}_{\mathbf{2}} + \mathbf{F}_{\mathbf{2}}^{\mathbf{uu}})\boldsymbol{B}_{\boldsymbol{y}}^{\mathbf{2}} \end{aligned} \tag{38}$$

If denote

$$\boldsymbol{\Lambda}_{\mathbf{c}}\mathbf{H}_{\mathbf{2n}} - \mathbf{H}_{\mathbf{2n}}\mathbf{C}_{\mathbf{2}} + \mathbf{F}_{\mathbf{2}}^{\mathbf{uu}} \stackrel{\text{def}}{=} \mathbf{R}_{\mathbf{2n}} \tag{39}$$

By taking the vectorization of both sides, we can get:

$$(\boldsymbol{\Lambda}_{\mathbf{c}} \otimes \mathbf{I} + \mathbf{I} \otimes \mathbf{C}_{\mathbf{2}}) * \mathrm{vec}(\mathbf{H}_{\mathbf{2n}}) + \mathrm{vec}(\mathbf{F}_{\mathbf{2}}^{\mathbf{uu}}) = \mathrm{vec}(\mathbf{R}_{\mathbf{2n}}) \tag{40}$$

So if matrix $\boldsymbol{\Lambda}_{\mathbf{c}} \otimes \mathbf{I} + \mathbf{I} \otimes \mathbf{C}_{\mathbf{2}}$ has full rank, then no matter what in the right hand side, we could pick an appropriate $\mathbf{H}_{\mathbf{2n}}$ to make the equation satisfied, which means all the second order terms would be eliminated i.e. $\mathbf{R}_{\mathbf{2n}} = \mathbf{0}$ by the normal form transformation $\boldsymbol{u} = \boldsymbol{y} + \mathbf{H}_{\mathbf{2n}}\boldsymbol{B}_{\boldsymbol{y}}^{\mathbf{2}}$**.**

However, in practice we have known that the normal form of Hopf bifurcation doesn't have second order terms, which means $\mathbf{R_{2n}} = \mathbf{0}$. So we could solve $\mathbf{H_{2n}}$ by solving the matrix equation:

$$\mathbf{\Lambda_c H_{2n} - H_{2n} C_2 + F_2^{uu} = 0} \tag{41}$$

After we calculated $\mathbf{H_{2n}}$, we need to update the 3rd and higher order terms brought by transformation $\boldsymbol{u} = \boldsymbol{y} + \mathbf{H_{2n}}\boldsymbol{B_y^2}$. So we just substitute this into (35). Since

$$\begin{aligned}\boldsymbol{B_u^2} &= \left(\boldsymbol{y} + \mathbf{H_{2n}}\boldsymbol{B_y^2}\right) \otimes \left(\boldsymbol{y} + \mathbf{H_{2n}}\boldsymbol{B_y^2}\right)\\ &= \boldsymbol{y} \otimes \boldsymbol{y} + (\mathbf{I} \otimes \mathbf{H_{2n}} + \mathbf{H_{2n}} \otimes \mathbf{I})\left(\boldsymbol{y} \otimes \boldsymbol{B_y^2}\right) + O(\boldsymbol{y^4})\\ &= \boldsymbol{B_y^2} + (\mathbf{I} \otimes \mathbf{H_{2n}} + \mathbf{H_{2n}} \otimes \mathbf{I})\boldsymbol{B_y^3} + O(\boldsymbol{y^4})\end{aligned} \tag{42}$$

And

$$\boldsymbol{B_u^3} = \boldsymbol{B_y^3} + O\left(\boldsymbol{y^5}\right) \tag{43}$$

Thus,

$$\dot{\boldsymbol{y}} = \mathbf{\Lambda_c}\boldsymbol{y} + \underbrace{\left(\mathbf{F_2^{uu}}(\mathbf{I} \otimes \mathbf{H_{2n}} + \mathbf{H_{2n}} \otimes \mathbf{I}) + \mathbf{F_{3c}^{u}}\right)}_{\mathbf{N_y^3}}\boldsymbol{B_y^3} + O(\boldsymbol{y^4}) \tag{44}$$

3.3 Cubic normal form calculations

Now we need to introduce another nonlinear transformation

$$\boldsymbol{y} = \boldsymbol{z} + \mathbf{H_{3n}}\boldsymbol{B_z^3} \tag{45}$$

in order to simplify the cubic terms in the normal form as much as possible. Substitute this transformation into (44) we will get:

$$\begin{aligned}\dot{\boldsymbol{z}} &= (\mathbf{I} + \mathbf{H_{3n}}D\boldsymbol{B_z^3})^{-1}\begin{pmatrix}\mathbf{\Lambda_c}\boldsymbol{z} + \mathbf{\Lambda_c H_{3n}}\boldsymbol{B_z^3} + \\ \mathbf{N_y^3}\boldsymbol{B_z^3} + O(\boldsymbol{z^4})\end{pmatrix}\\ &= \mathbf{\Lambda_c}\boldsymbol{z} + \left(\mathbf{\Lambda_c H_{3n}}\boldsymbol{B_z^3} + \mathbf{N_y^3}\boldsymbol{B_z^3} - \mathbf{H_{3n}}D\boldsymbol{B_z^3}\mathbf{\Lambda_c}\boldsymbol{z}\right) + \boldsymbol{O}(\boldsymbol{z^4})\end{aligned} \tag{46}$$

We can denote $D\boldsymbol{B_z^3}\mathbf{\Lambda_c}\boldsymbol{z} \stackrel{\text{def}}{=} \mathbf{C_3}\boldsymbol{B_z^3}$, where

$$\mathbf{C_3} = \left(\mathbf{I_{n^2}} \otimes \mathbf{\Lambda_c}\right) + \mathbf{I_n} \otimes \begin{bmatrix}\mathbf{I_n} \otimes \boldsymbol{\Lambda_{c1}}\\ \vdots \\ \mathbf{I_n} \otimes \boldsymbol{\Lambda_{cn}}\end{bmatrix} + \begin{bmatrix}\mathbf{I_{n^2}} \otimes \boldsymbol{\Lambda_{c1}}\\ \vdots \\ \mathbf{I_{n^2}} \otimes \boldsymbol{\Lambda_{cn}}\end{bmatrix} \tag{47}$$

So the 3rd order terms after the transformation is:

$$\begin{aligned}&\mathbf{\Lambda_c H_{3n}}\boldsymbol{B_z^3} + \mathbf{N_y^3}\boldsymbol{B_z^3} - \mathbf{H_{3n}}D\boldsymbol{B_z^3}\mathbf{\Lambda_c}\boldsymbol{z} =\\ &\left(\mathbf{\Lambda_c H_{3n} - H_{3n}C_3 + N_y^3}\right)\boldsymbol{B_z^3} \stackrel{\text{def}}{=} \mathbf{R_{3n}}\boldsymbol{B_z^3}\end{aligned} \tag{48}$$

Similar to quadratic normal form transformation, we take the vectorization of both sides:

$$(\mathbf{\Lambda_c} \otimes \mathbf{I} + \mathbf{I} \otimes \mathbf{C_3}) * \mathrm{vec}(\mathbf{H_{3n}}) + \mathrm{vec}\left(\mathbf{N_y^3}\right) = \mathrm{vec}(\mathbf{R_{3n}}) \tag{49}$$

Now our goal is to come up with an appropriate $\mathbf{H_{3n}}$ to simplify $\mathbf{N_y^3}$ into $\mathbf{R_{3n}}$, which is the normal form we need. Interestingly, we have known what the normal form looks like, for example, the Hopf normal form is shown in (9). Since we have known that the 3rd order terms cannot be all eliminated, and we know the column basis of $\mathrm{vec}(\mathbf{R_{3n}})$, so we could easily find the coefficient of the normal forms by solving this equation [5].

3.4 Computations Summary

The computational framework presented in this section shows how center manifold computations and normal form calculations can be carried out for analyzing Hopf bifurcations for large nonlinear systems such as the power system. Computational complexity comes from the need for evaluating higher order derivatives (up to third order) and computing many Kronecker products of matrices.

4. Numerical Examples

In this section, we will be using the 2-area-11-bus-4-machine Kundur system to illustrate the computational process and the challenges that we encountered for finding the 3rd order Hopf normal form coefficient. We will show how the Hopf bifurcation can change from one type to the other (subcritical versus supercritical) as we change the system parameters. Also we will show the different system behavior associated with the two different types.
The one-line diagram of the system is shown below, where the line resistance and reactance and the shunt capacitor at bus 7 and 9 can be found in [1].

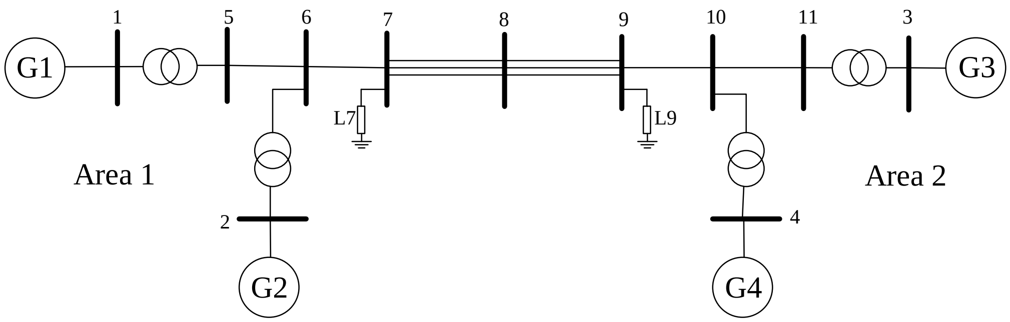

Figure 4.1 One-line diagram of the Kundur test system

In this system, we have represented the generators with two-axis flux decay machine models each equipped with an ESAC1A exciter and a TGOV1 governor. In general, power system dynamics is modeled by differential equations describing the system dynamics along with a set of algebraic equations defined by the system power flow solutions [1]. However, for our computational convenience, we prefer to have a system model in the form of ordinary differential equations (1). Accordingly, we assume the generator parameters $x_d' = x_q'$ to ignore saliency effects. Also, the two loads in the system are modeled by constant impedance load types. With these assumptions, we can perform network reduction to eliminate the algebraic power-flow equations from the system model. Now the whole system can be described by a set of ordinary differential equations.
The generator equations are:

$$\begin{cases} T_{di}'\dot{E}_{qi}' = -E_{qi}' - (X_{di} - X_{di}')I_{di} + E_{fdi} \\ T_{qi}'\dot{E}_{di}' = -E_{di}' + \left(X_{qi} - X_{qi}'\right)I_{qi} \\ \dot{\delta}_i = \omega_i - \omega_s \\ 2H_i\dot{\omega}_i = P_{mi} - \left(E_{qi}'I_{qi} + E_{di}'I_{di}\right) - D_i(\omega_i - \omega_s) \end{cases} \tag{50}$$

where $\omega_s = 120\pi$, $I_{di} = \frac{E_{qi}' - V_{qi}}{X_{di}'}$, $I_{qi} = -\frac{E_{di}' - V_{di}}{X_{qi}'}$

T

he exciter equations of ESAC1A are:

$$\begin{cases} T_{fi}\dot{V}_{fi} = V_{fei} - V_{fi} \\ T_{ai}\dot{V}_{ai} = V_{refi} - \sqrt{V_{di}^2 + V_{qi}^2} - \frac{K_{fi}}{T_{fi}}\left(V_{fei} - V_{fi}\right) - V_{ai} \\ T_{ei}\dot{V}_{ei} = K_{ai}V_{ai} - V_{fei} \end{cases} \tag{51}$$

where $V_{fei} = K_{di}I_{fdi} + K_{ei}V_{ei}$, $I_{fdi} = E_{qi}' + (X_{di} - X_{di}')I_{di}$ and $E_{fdi} = V_{ei} - 0.577K_{ci}I_{fdi}$

The governor equations of TGOV1 are:

$$\begin{cases} T_{1i}\dot{V_{g1i}} = P_{refi} - \dfrac{\omega_i}{\omega_s R_i} - V_{g1i} \\ T_{3i}\dot{V_{g2i}} = V_{g1i} - V_{g2i} \end{cases} \tag{52}$$

where $P_{mi} = \left(1 - \frac{T_{2i}}{T_{3i}}\right) V_{g2i} + \frac{T_{2i}}{T_{3i}} V_{g1i} - \frac{D_{ti}\omega_i}{\omega_s}$

In the above equations, the subscript $i = 1, \dots, 4$ denotes each of the four generators. V_{di} and V_{qi} are connected to state E'_{di} and E'_{qi} by the reduced network admittance matrix $\mathbf{Y_{red}}$ which we precomputed:

$$V_{di} + jV_{qi} = \mathbf{Y_{red}} * \left(E'_{di} + jE'_{qi}\right) \tag{53}$$

Our computations and analysis will start from here.

4.1 Supercritical case

In this case, the generator output and load consumption are summarized in Table below:

Table 4.1 Generator output and load consumption in supercritical case

	P(MW)	**Q(MW)**
G1	461.473	1.853
G2	500.423	46.784
G3	719.0	97.513
G4	700.0	71.103
L7	967.0	100.0
L9	1367.0	100.0

The parameters of generators and ESAC1A exciters and TGOV1 governors are shown in Table below. The values are in per unit values in machine MVA base. The parameters for the four generators are the same, except for the generator inertia H (6.5 for G1 and G2, 6.175 for G3 and G4).

Table 4.2 Machine parameters in the supercritical case

GEN	T'_d	T'_q	H	D	X_d
	8	0.4	6.5(6.175)	1.0	1.8
	X_q	X'_d	X_l	R_s	**MBASE**
	1.7	0.45	0.18	0	900
ESAC1A	K_A	T_A	T_E	K_F	T_F
	192.0	0.2	0.8	0.3	1.0
	K_C	K_D	K_E		
	0.2	0.38	0.1		
TGOV1	**R**	T_1	T_2	T_3	D_t
	0.05	10.0	1.0	1.0	0.0

With the knowledge of these parameters, we could easily solve the power-flow and perform dynamic state initialization of the system. Then we could eliminate the power flow equations by network reduction, where we will end up with a set of ordinary differential equations. If there is no angle reference, the system Jacobian matrix will have a zero eigenvalue. This will bring some inconvenience to our further analysis, so we choose δ_4 as the angle reference in the system to eliminate this extra degree of freedom.

By linearization around the equilibrium point, the system Jacobian matrix has a pair of complex conjugate eigenvalues on the imaginary axis: $\pm j3.74$, which is the inter-area mode of the system at frequency 0.59Hz. All the other modes of the system have negative real parts, i.e. in the open left half complex plane.

Then by performing the center manifold computation outlined in previous section, we get:

$$\begin{bmatrix}\dot{u_1}\\ \dot{u_2}\end{bmatrix} = \underbrace{\begin{bmatrix}0 & -3.74\\ 3.74 & 0\end{bmatrix}}_{\mathbf{\Lambda_c}}\begin{bmatrix}u_1\\ u_2\end{bmatrix} +$$
$$\underbrace{\begin{bmatrix}-0.030 & -0.759 & -0.780\\ -0.033 & -0.099 & -0.767\end{bmatrix}}_{\mathbf{F_2^{uu}}}\begin{bmatrix}u_1^2\\ u_1u_2\\ u_2^2\end{bmatrix} +$$
$$\underbrace{\begin{bmatrix}-0.068 & -0.960 & -1.122 & 1.447\\ -0.077 & -0.045 & 0.265 & 0.069\end{bmatrix}}_{\mathbf{F_{3c}^{u}}}\begin{bmatrix}u_1^3\\ u_1^2u_2\\ u_1u_2^2\\ u_2^3\end{bmatrix} + O(u^4) \tag{54}$$

Here we write $\mathbf{\Lambda}_c$ into skew symmetric matrix because we want to get rid of the complex values in the matrix entries, but it should be noted that this is equivalent to a diagonal matrix with just an easy linear transformation. Now original 35-dimensional system is reduced to a 2-dimensional system.

Our next step is to simplify this system using normal form theory. We first simplify the second order terms $\mathbf{F_2^{uu}}$ by $\mathbf{H_{2n}}$:

$$\mathbf{H_{2n}} = \begin{bmatrix}0.207 & 0.125 & 0 & 0.006\\ -0.133 & 0.199 & 0 & -0.084\end{bmatrix} \tag{55}$$

Then, $\mathbf{R_{2n}} = \mathbf{0}$. Then we can get $\mathbf{N_y^3}$**:**

$$\mathbf{N_y^3} = \begin{bmatrix}0.021 & -1.069 & -1.464 & 1.573\\ -0.077 & 0.110 & -0.044 & 0.197\end{bmatrix} \tag{56}$$

Our last step is to calculate $\mathbf{H_{3n}}$ and $\mathbf{R_{3n}}$ to simplify the third order terms into the standard Hopf bifurcation normal form as we shown in (9). Finally, we got the normal form:

$$\begin{cases}\dot{r} = \mu r - 0.088r^3\\ \dot{\theta} = 3.74 + O(r^2)\end{cases} \tag{57}$$

where μ is determined by the real part of the eigenvalue. In the normal form, $a = -0.088 < 0$, so we conclude that this is a supercritical Hopf bifurcation.

Then we will look at the system behavior as the critical eigenvalue transverses across the imaginary axis from left to right. We will show the effect of variation of system parameter by tuning the generator output and the exciter gains.

4.1.1 Change in generator output

We set $P_{g2} = 520\text{MW}$ where $\mu = -0.005$. The normal form tells us the equilibrium is stable and there are no limit cycles surrounding it. If we simulate a disturbance on the system, the system behavior is as shown in Figure 2.1. As predicted by the normal form, the system trajectory will converge back to the equilibrium point. However, if we set $P_{g2} = 480\text{MW}$ where $\mu = 0.005$. Now the equilibrium point is unstable, and there is a stable limit cycle surrounding it. By simulating a disturbance on the system, we can see the oscillation magnitude of generator speed keeps increasing until the trajectory converges to the stable limit cycle (Figure 4.3). Temporary operation at such a stable limit cycle may be acceptable as long as the oscillation amplitudes are not large. In this sense, the case of supercritical Hopf bifurcation is less disruptive to system operation in that the steady state operation changes from a stable equilibrium point (Figure 4.2) to a stable limit cycle (Figure 4.3).

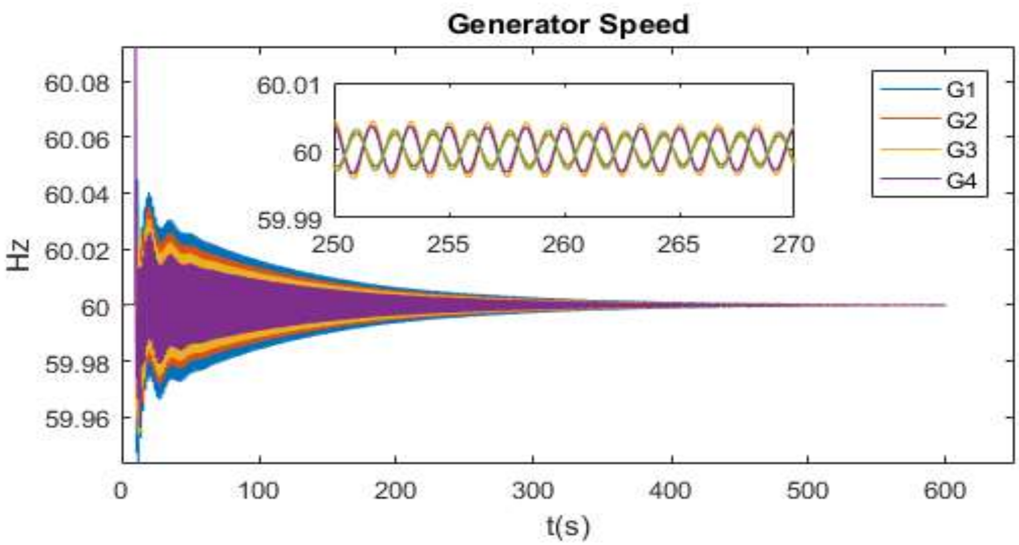

Figure 1.2 Supercritical case with $\mu < 0$ (P_{g2} = 520MW), convergence to stable equilibrium point.

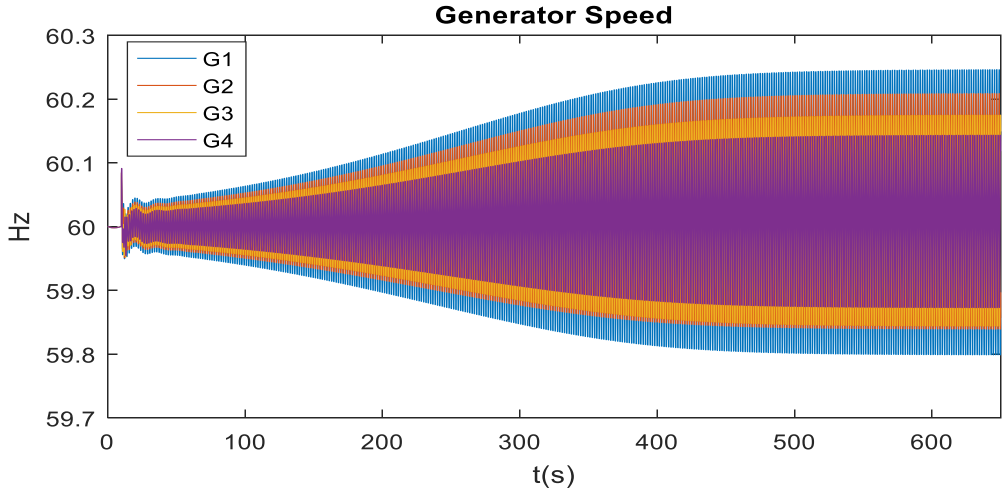

Figure 4.3 Supercritical case with $\mu > 0$ (P_{g2} = 480MW), convergence to stable limit cycle.

4.1.2 Change in exciter gains

Now we change the exciter gains to see its effect on the real part of the critical eigenvalue. By changing $K_A = 184$ to $K_A = 200$, μ changes from $\mu = 0.004$ to $\mu = -0.004$. If we place the same disturbance for two cases, the four generator speeds are shown in figures below. A stable limit cycle (Figure 4.4) and a stable equilibrium point (Figure 4.5) can be clearly seen for two different parameter settings.

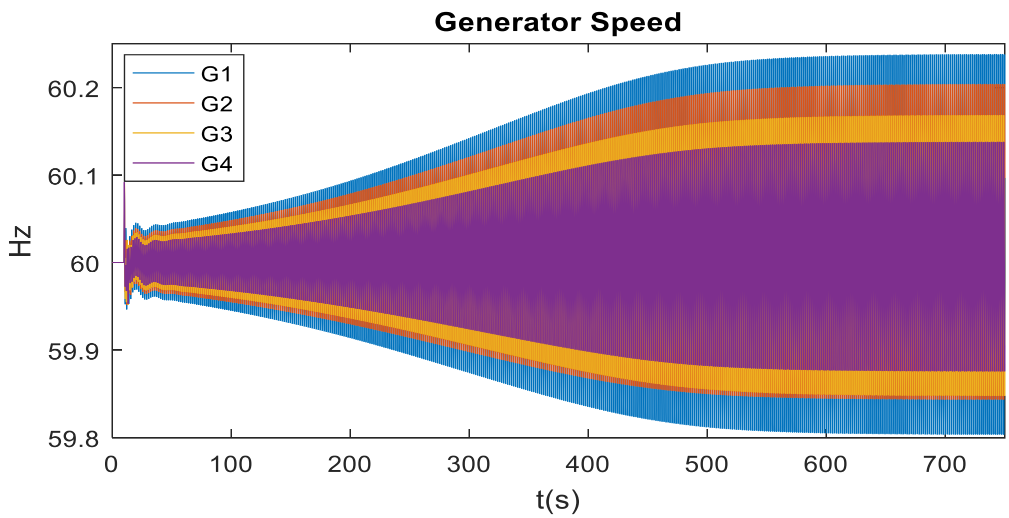

Figure 4.4 Supercritical case with $\mu > 0$ ($K_A = 184$), convergence to stable limit cycle.

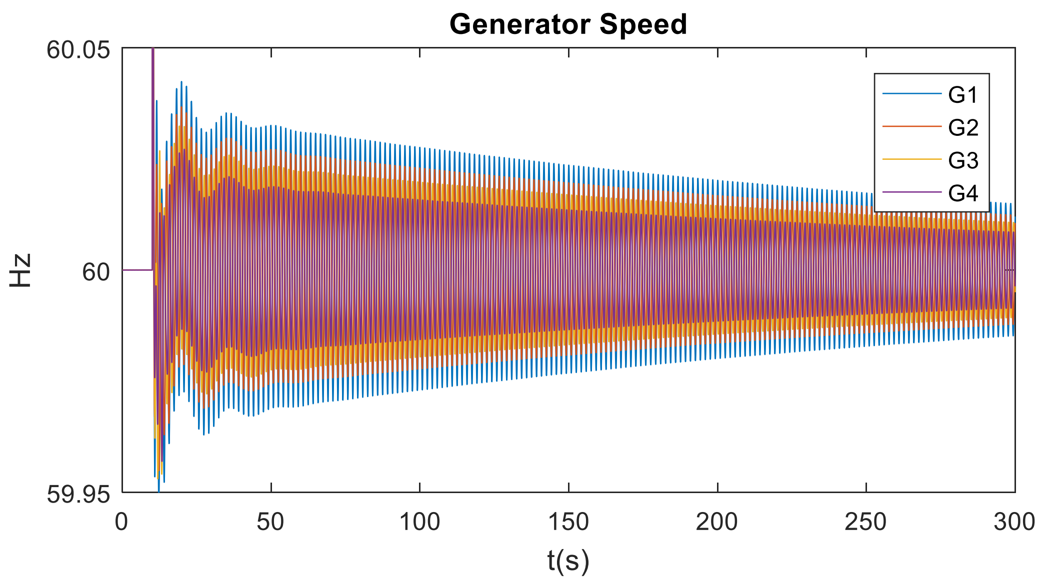

Figure 4.5 Supercritical case with $\mu < 0$ ($K_A = 200$), convergence to stable equilibrium point.

4.2 Subcritical case

By tuning the generator output, load consumption and exciter parameters into the following values shown in Table and Table 4, we get a subcritical Hopf bifurcation in the system. The system has a pair of eigenvalues at $\pm$j3.23.

Table 4.3 Generator outputs and load consumptions for the subcritical case

	P(MW)	**Q(MW)**
G1	688.322	133.624
G2	784.295	301.381
G3	750.0	172.597
G4	700.0	234.302
L7	967.0	100.0
L9	1867.0	100.0

Table 4.4 Exciter parameters for the subcritical case

ESAC1A	$\boldsymbol{K_A}$	$\boldsymbol{T_A}$	$\boldsymbol{T_E}$	$\boldsymbol{K_F}$	$\boldsymbol{T_F}$
	35	0.02	0.8	0.03	1.0
	$\boldsymbol{K_C}$	$\boldsymbol{K_D}$	$\boldsymbol{K_E}$		
	0.2	0.38	1.0		

By applying the same process, normal form of this system is:

$$\begin{cases} \dot{r} = \mu r + 0.009 r^3 \\ \dot{\theta} = 3.23 + O(r^2) \end{cases} \tag{58}$$

This is a subcritical Hopf case. Then we will look at the system behavior as the critical pair of eigenvalues transverse across the imaginary axis from left to right.

4.2.1 Change in generator output

Now we will change the active power output of G3 to see its effects on the system behavior. By changing it from $P_{g3} = 730MW$ to $P_{g3} = 770MW$, μ changes from $\mu = 0.0058$ to $\mu = -0.0044$. By simulating a small disturbance on the system, the system diverges when $\mu > 0$ (Figure 4.6) while it converges back to equilibrium point when $\mu < 0$ (Figure 4.7). However, when $\mu < 0$, as we increase the fault-on-time of the disturbance, we can see the presence of an unstable limit cycle which leads to eventual divergence in Figure 4.8. It can be shown that the unstable limit cycle anchors the boundary of region of attraction for the stable equilibrium in this case [8]. Unlike the case of supercritcal Hopf bifurcation (Figure 4.3), the system trajectory will lead to divergence (Figure 4.6) and possible system disruption in the case of subcritical Hopf bifurcation because of the disappearance of the region of attraction. Therefore, the occurrence of subcritical Hopf bifurcation is more problematic for the sustained acceptable operation of the power grid when compared with the occurrence of supercritical Hopf bifurcation.

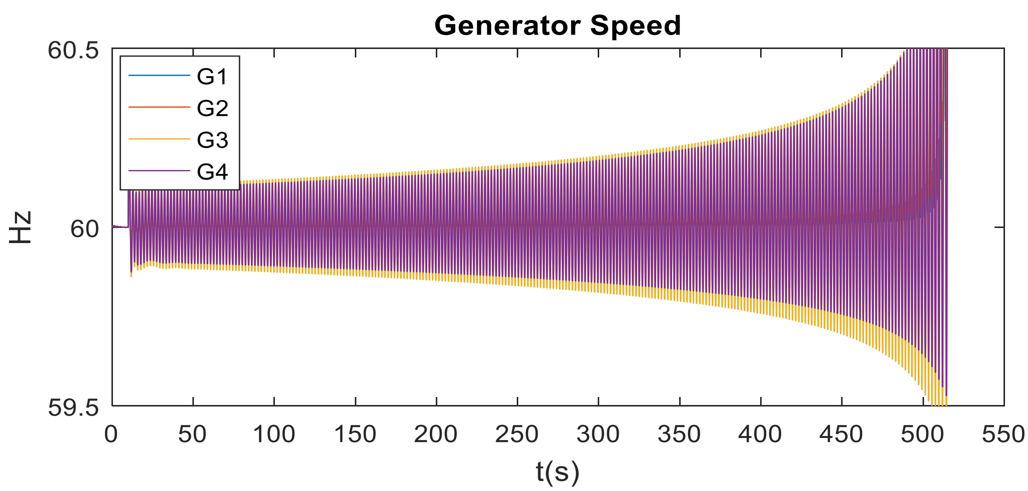

Figure 4.6 Subcritical case with $\mu > 0$ ($P_{g3} = 730MW$), divergence.

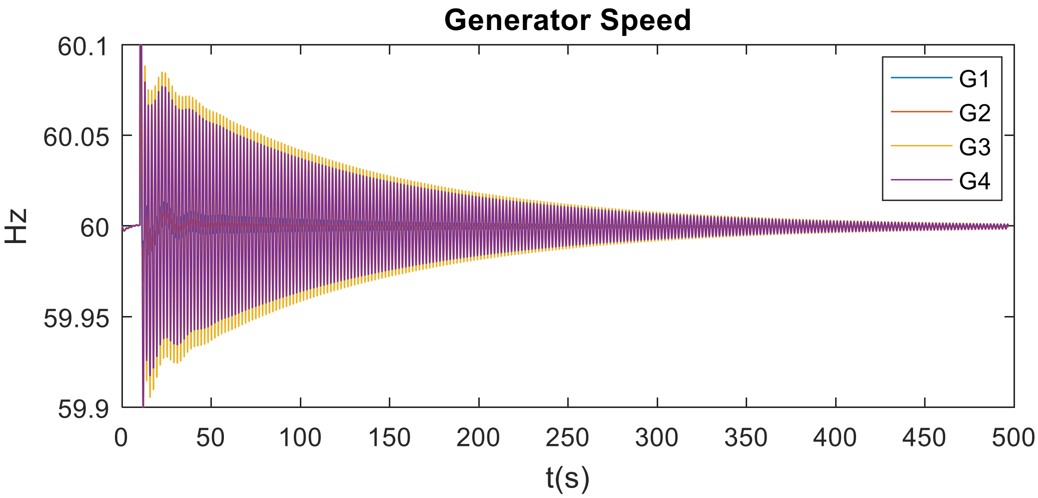

Figure 4.7 Subcritical case with $\mu < 0$ ($P_{g3} = 770MW$), "inside" unstable limit cycle leads to convergence to stable equilibrium point.

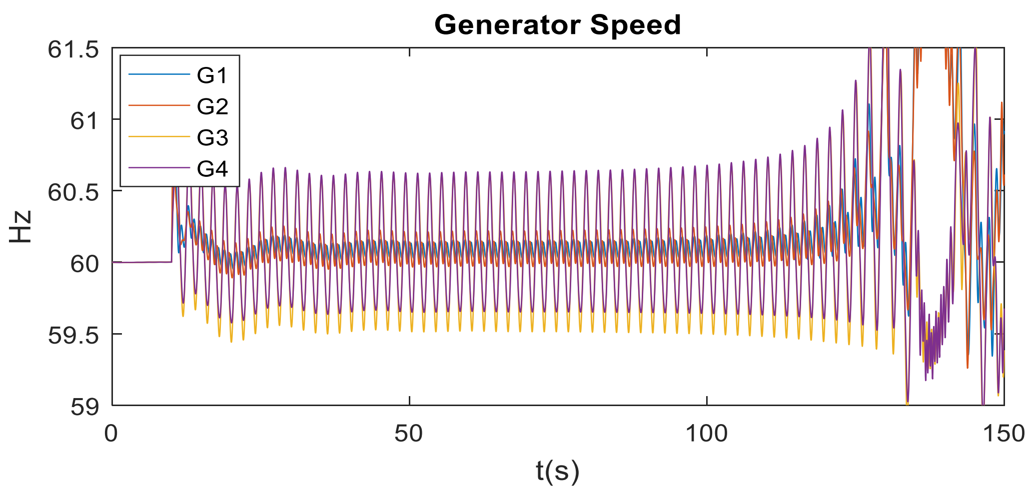

Figure 4.8 Subcritical case with $\mu < 0$ ($P_{g3} = 770MW$), "outside" unstable limit cycle leads to divergence

4.2.2 Change of exciter gains

By setting exciter gain of all exciters to $K_A = 37$, we get $\mu = 0.016$. Based on the normal form, the equilibrium point is unstable, and there is no limit cycle surrounding it. By playing a disturbance on the system, we could see the system trajectory will diverge from the equilibrium point until collapse (Figure 4.9). Then we change the exciter gain to $K_A = 33$, we get $\mu = -0.015$. Now the equilibrium is stable but there is an unstable limit cycle surrounding it. By simulating a disturbance on the system, we can see as the fault on time is shorter i.e. 2 cycles in Figure 4.10, the system will converge back to the equilibrium point; while the fault on time is longer i.e. 12 cycles in Figure 4.11, the system trajectory will diverge from the unstable limit cycle. So the unstable limit cycle can be taken as the stability boundary of the stable equilibrium point.

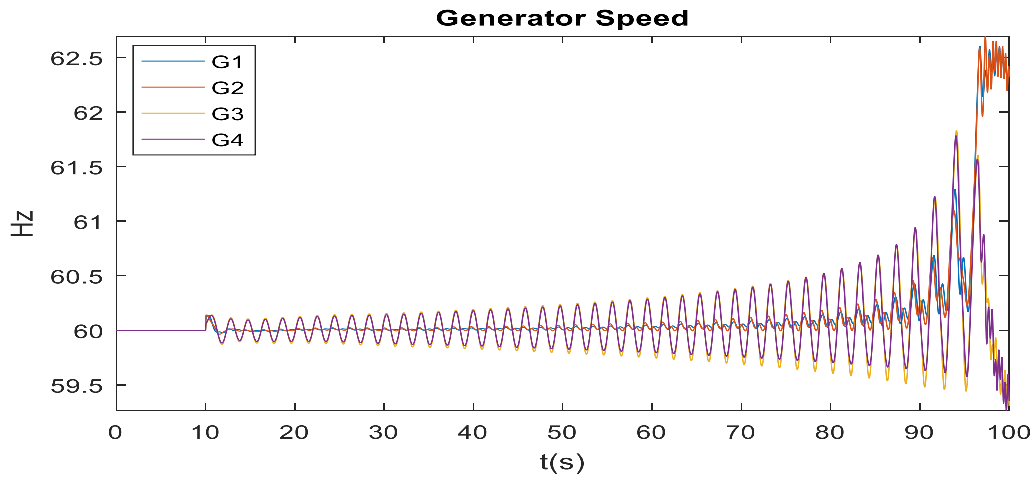

Figure 4.9 Subcritical case with $\mu > 0$ ($K_A = 37$), divergence.

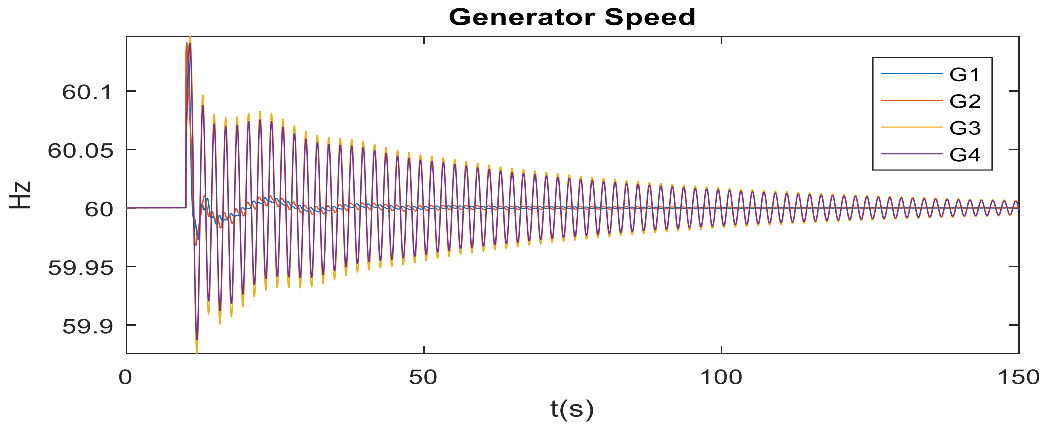

Figure 4.10 Subcritical case with $\mu < 0$ ($K_A = 33$, "inside" unstable limit cycle leads to convergence to stable equilibrium point.

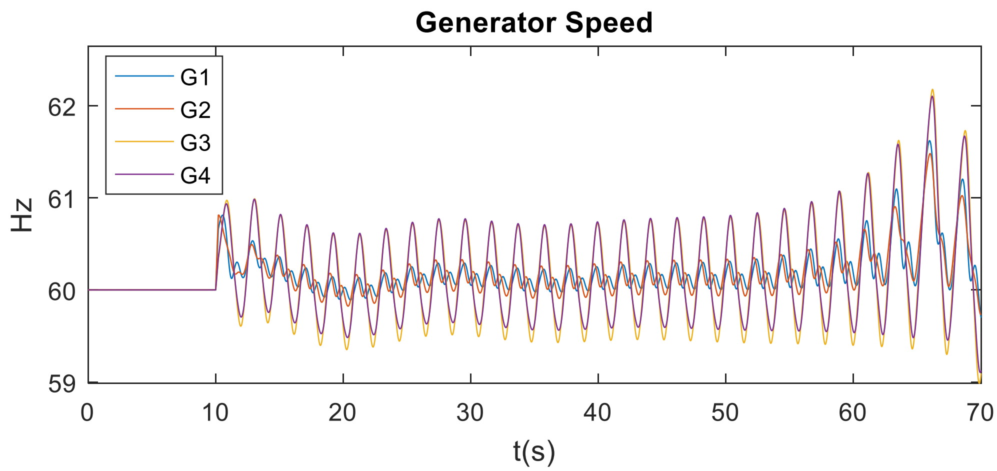

Figure 4.11 Subcritical case with $\mu < 0$ ($K_A = 33$), "outside" unstable limit cycle leads to divergence.

4.3 Transition between Supercritical and Subcritical as Parameter Changes

In this section, we provide a series of cases showing as the system parameter changes, how supercritical cases will change into subcritical and vice versa [8].

We start from the supercritical case in Section A, then we keep decreasing the exciter gains K_A of all four exciters. At the same time, we tune the generator active power output P_{G2} of generator at bus 2 to "place" the eigenvalues on the imaginary axis thus resulting in Hopf bifurcations. The "a" coefficients are calculated during this process and is summarized in the

Table below:

Table 4.5 Coefficient "a" under parameter variations

K_A	$P_{G2}(MW)$	a
192	500.423	-0.0877
190	504.273	-0.0793
180	525.918	-0.0492
170	553.168	-0.0253
160	589.838	-0.0065
150	643.470	0.0091
145	681.832	0.0175
140	748.122	0.0364

As we can see from the table, as K_A decreases and P_{G2} increases correspondingly, the coefficient "a" is increasing and eventually changes from negative to positive. This means that supercritical Hopf has gradually transitioned into subcritical Hopf as the system parameters change. From the previous time domain simulations, we know that supercritical and subcritical cases will behave very differently when the equilibrium point becomes unstable. In a real power system whose parameter space could be very large, distinguishing between these two cases will help system operators choose the right remedial action when system gets close to instability, that is, when a complex conjugate mode becomes poorly damped.

Furthermore, we could use this case to study the interactions of stable and unstable limit cycles resulting from supercritical and subcritical Hopf bifurcations as shown in Figure 4.12. The system dynamics is influence by three different limit cycles, two unstable and one stable limit cycle in this case. We have a subcritical Hopf bifurcation when the exciter gains are at 145, where the inner unstable limit cycle shrinks down in size to zero and disappears. Then we have a supercritical Hopf bifurcation when exciter gains are equal to 42, where the stable limit cycle collapses down and disappears. Moreover, outside the inner unstable and stable limit cycles, there is another unstable limit cycle. The example shows the complex dynamics of the system in the parameter space. In terms of more detailed analysis of these nested limit cycles, we may need to compute fifth order normal form coefficients, which is beyond the scope of this report. We plot a phase plane plot of active power on interface 8-9 vs. frequency from generator at bus 3 in

Figure 4.13 for summarizing a snapshot of the system dynamics near the equilibrium point when the exciter gains equal 170 in Figure 4.12. We can see the stable equilibrium point O is surrounded by three limit cycles. If the initial condition is inside the stability boundary anchored by the unstable limit cycle γ_1, the system trajectory will converge to the equilibrium O; if it is outside the boundary anchored by γ_1, the trajectory will converge to stable limit cycle γ_2; if the initial condition is outside of the stability boundary associated with γ_1 but inside the boundary anchored by the unstable limit cycle γ_3, then it will converge back to the stable limit cycle γ_2; if it is outside the boundary associated with γ_3, the dynamics will diverge eventually.

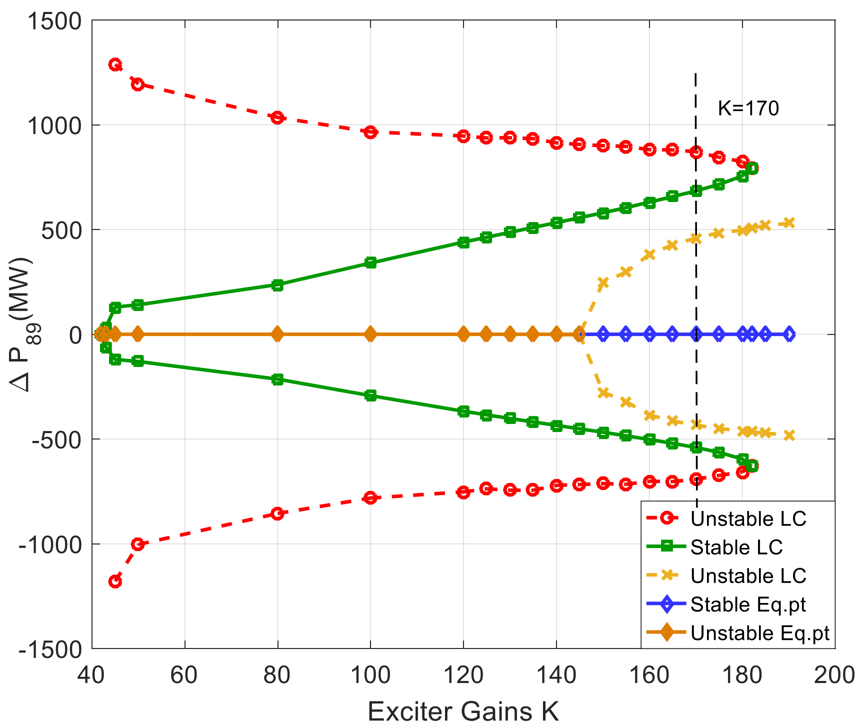

Figure 4.12 Limit cycle magnitude in ΔP_{8-9} vs. exciter gains K

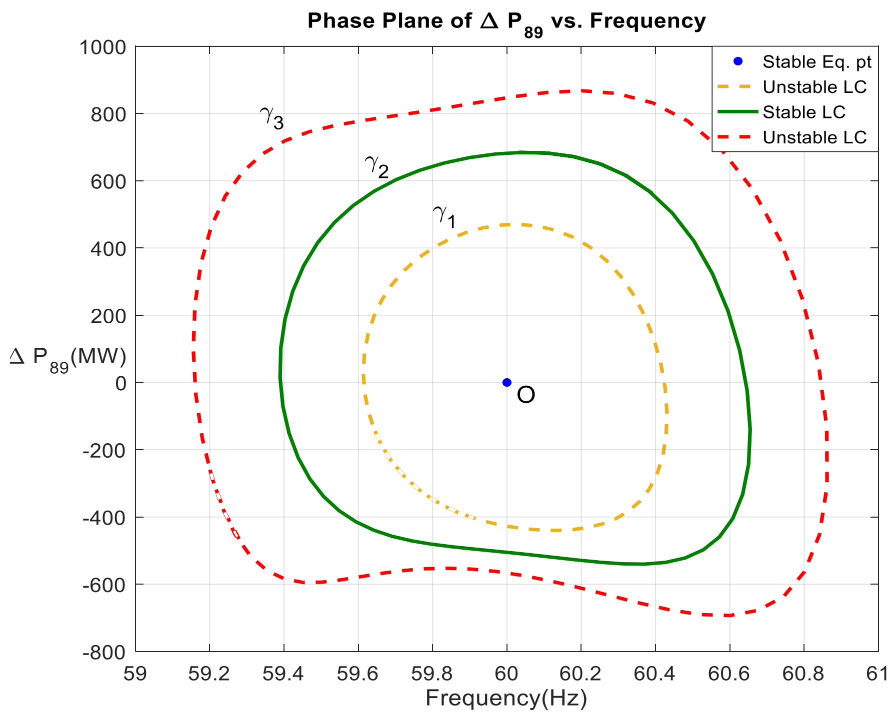

Figure 4.13 Phase plane projection of the limit cycles for $K = 170$

5. Discussion

In this report, we have proposed a systematic process for analyzing Hopf bifurcations in power system. By applying center manifold and normal form theory, we have systematically reduced complex nonlinear analysis into evaluation of high order derivatives and matrix computations. By calculating the third order coefficient in the normal form, we can directly know if a Hopf bifurcation is supercritical or subcritical Hopf. This will largely help us to understand and predict the system trajectory behavior as the real part of the system eigenvalues changes its sign, which will lead to birth or disappearance of stable or unstable limit cycles surrounding the system equilibrium point. In this context, supercritical Hopf bifurcations may be less harmful in the sense that temporary operation at stable limit cycles with low oscillation amplitudes may be tolerable and may buy system operators some time to take corrective actions. On the other hand, subcritical Hopf bifurcations need urgent attention to stay away from low damping conditions for that mode. Further research is indicated on analysis of transitions between the two types and on the implications of nested limit cycles for general power system models.

References

[1] P. Kundur, *Power system stability and control*, McGraw-hill, 1994.

[2] Guckenheimer J., Holmes P, Nonlinear Oscillations, Dynamical Systems, and Bifurcations of Vector Fields. Applied Mathematical Sciences, vol 42. Springer, New York, NY, 1983.

[3] S. Wiggins, Introduction to applied nonlinear dynamical systems and chaos. New York: Springer, 2003.

[4] E. H. Abed, and P. P. Varaiya "Nonlinear oscillations in power systems" Int. J. Electric Power Energy Syst. vol. 6 pp. 37-43 1984.

[5] W. Ji, "Analysis of Complicated Oscillatory Instability Phenomena in General Power System Models," Ph.D. dissertation, Dept. Electrical. Eng., Washington State Univ., Pullman, WA, USA, 1997.

[6] W. Ji and V. Venkatasubramanian, “Center manifold computations in bifurcation analysis of large systems such as the power system,” Proceedings of 1995 American Control Conference - ACC95.

[7] V. Venkatasubramanian and W. Ji, “Numerical Approximation of (N - 1)-Dimensional Stable Manifolds in Large Systems Such as the Power System,” IFAC Proceedings Volumes, vol. 29, no. 1, pp. 7093–7098, 1996.

[8] V. Venkatasubramanian, H. Schattler and J. Zaborszky, "Local bifurcations and feasibility regions in differential-algebraic systems," in *IEEE Transactions on Automatic Control*, vol. 40, no. 12, pp. 1992-2013, Dec. 1995.

[9] F. Howell and V. Venkatasubramanian, "A modal decomposition of the Hopf normal form coefficient," in *IEEE Transactions on Automatic Control*, vol. 46, no. 7, pp. 1080-1083, July 2001.